Supporting Information

Structural basis for enhancement of carbapenemase activity in the OXA-51 family of class D β-lactamases

Clyde A. Smith[1*], Nuno Tiago Antunes[2], Nichole K. Stewart[2], Hilary Frase[2], Marta Toth[2], Katherine A. Kantardjieff[3], and Sergei B. Vakulenko[2*]

[1] Stanford Synchrotron Radiation Lightsource, Stanford University, Menlo Park, CA, USA

[2] Department of Chemistry and Biochemistry, University of Notre Dame, Notre Dame, IN, USA

[3] College of Science and Mathematics, California State University, San Marcos, CA, USA

METHODS

Cloning

For MIC determination, the gene encoding the class D β-lactamase OXA-51 from *Acinetobacter baumannii* (GenBank accession number ABD47672.1) was custom synthesized and cloned into the unique NdeI-HindIII restriction sites of the shuttle vector pNT221.[1] The vector encoding the OXA-51 gene was subsequently transformed into *E. coli* JM83 by chemical transformation and into *A. baumannii* ATCC 17978 by electroporation. For protein purification, the gene sequence was optimized for expression in *E. coli* and synthesized. The signal peptide, predicted to be comprised of first 17 amino acids, was removed and replaced by a methionine codon. The gene encoding mature OXA-51 was cloned into the NdeI and HindIII restriction sites of the pET24a(+) vector (Invitrogen) and transformed into *E. coli* BL21 (DE3) competent cells for protein production.

Mutagenesis

The Trp222Met variant of OXA-51 was obtained by site directed mutagenesis of the wild-type sequence. Briefly, two oligonucleotide primers were used to amplify the entire pNT221plasmid containing the gene for OXA-51. In one of these primers, the codon for tryptophan was substituted with that for methionine. The resulting PCR product was digested for one hour with DpnI, gel purified and self-ligated with T4 DNA ligase for one hour. The ligation product was used to transform chemically competent *E. coli* JM83. Transformed cells were incubated overnight at 37 ºC in LB broth supplemented with 60 μg/ml kanamycin, and the

plasmid DNA was extracted and digested with NdeI-HindIII. The resulting fragment was religated into the NdeI-HindIII restriction sites of the vectors pNT221 and pET24a(+) and used for further experiments.

Purification of the OXA-51and OXA-51:Trp222Met β-lactamases

Five milliliters of an overnight culture of *E. coli* BL21 (DE3) harboring the pET24a(+) vector with the gene for OXA-51 or its Trp222Met mutant were used to inoculate 500 ml of fresh LB broth supplemented with 60 μg/ml of kanamycin. The cells were grown at 37 ºC with shaking (180 rpm) until an OD_{600} value of 0.8 was reached. The protein expression was induced by the addition of isopropyl β-D-thiogalactopyranoside (IPTG) to a final concentration of 1 mM. Next, the temperature was decreased to 22 ºC and the cells were incubated for an additional 20 hours with shaking (180 rpm). The cells were pelleted by centrifugation at 8,000 × *g* for 30 minutes at room temperature, resuspended in 10 mM Tris pH 7.0 and disrupted by sonication. The resulting cell lysate was centrifuged at 18,000 × *g* for 1 hour at 4 ºC. The supernatant was loaded onto a High Q anion-exchange column (BioRad) equilibrated in the same buffer. At this pH, the enzyme does not bind to this resin and was recovered in the flow through. The resulting fractions were analyzed by SDS-PAGE and their activity towards nitrocefin was determined. The fractions containing the protein were pooled and dialyzed against 20 mM HEPES pH 7.5. The protein was ≥ 95% pure as judged by SDS-PAGE visualization and the yield was approximately 400 mg of protein per liter of culture.

Enzyme kinetics

Kinetic data were collected using a Cary 60 spectrophotometer (Agilent). Reactions were performed at 22 °C in the presence of 2.5-100 μM carbapenem in 100 mM sodium phosphate buffer, pH 7.0 supplemented with 50 mM sodium bicarbonate and 0.2 mg/ml bovine serum albumin (BSA) and were initiated by adding various amounts of enzyme. The absorbance was monitored using the following conditions: imipenem (λ = 297 nm and Δε = -10,930 M^{-1} cm^{-1}), meropenem (λ = 298 nm and Δε = -7,200 M^{-1} cm^{-1}), ertapenem (λ = 295 nm and Δε = -10,940 M^{-1} cm^{-1}) and doripenem (λ = 297 nm and Δε = -11,540 M^{-1} cm^{-1}). The steady-state velocities (v) were calculated from the linear portion of each reaction time course and were used to determine the observed rate constants ($k_{obs} = v/[E]$), where E is the enzyme concentration. The steady-state parameters k_{cat} and K_m were determined by plotting k_{obs} as a function of the carbapenem concentration and fitting the data non-linearly to the Michaelis-Menten equation using Prism 6 (GraphPad Software, Inc.). Data were collected from at least three independent experiments.

Crystallization and Data Collection

The protein was concentrated to 25 mg/ml prior to setting up initial crystallization trials as sitting drops in Intelliplates, using PEG/Ion screens I and II, and Crystal Screens I and II (Hampton Research). After several days, showers of crystals were observed in condition 23 (0.2 M magnesium chloride hexahydrate, 0.1 M HEPES sodium, pH 7.5, 30% PEG400) from Crystal Screen I. Crystals were improved using seeding techniques and were flash cooled in a

cryoprotectant comprising the crystallization mother liquor augmented with 25% glycerol. The crystals diffracted to approximately 2.0 Å resolution and belonged to the primitive tetragonal space group I422 with cell dimensions a = b = 131.11 Å, c = 67.53 Å. The Matthews coefficient[2] assuming one molecule in the asymmetric unit was 2.35 $Å^3$/Da (48% solvent content). A complete dataset comprising 400 images with a rotation angle of 0.25° was collected from a single crystal on beamline BL12-2 at the Stanford Synchrotron Radiation Lightsource (SSRL) using x-rays at 13000 eV (0.9537 Å) and a PILATUS 6M PAD detector running in shutterless mode. The data were processed with XDS [3] and processed and scaled with POINTLESS and AIMLESS from the CCP4 suite of programs.[4] Final data collection statistics are given in Table S3.

Structure Solution and Refinement

The OXA-51 sequence was aligned with the three other class D carbapenemases whose structures had been determined, giving pairwise sequence identities of 57.5%, 61.9% and 50.0% for OXA-23 (PDB code 4JF4), OXA-24 (PDB code 3G4P) and OXA-58 (PDB code 4OH0). The structure of OXA-24 from *A. baumannii* was chosen as the starting model for molecular replacement (MR). All solvent molecules were removed from the OXA-24 model prior to MR calculations, and the CCP4 program CHAINSAW was used to convert OXA-24 into a pseudo-OXA-51 model, whereby identical residues in the two sequences were retained and those which differed were truncated at the Cβ atom. A strong MR solution gave the position of the single OXA-51 molecule. Refinement of the structure was completed with the PHENIX suite of programs,[5] and manual building of the model using the molecular graphics program COOT.[6]

Water molecules were added in structurally to chemically relevant positions. Final refinement statistics are given in Table S4.

Superpositions were performed using the SSM procedure[7] as implemented in COOT,[6] and the program LSQKAB in the CCP4 suite.[4] Structural figures were prepared using PYMOL.[8]

Flexible Docking and Energy Minimization

An initial position for meropenem in OXA51 was established by superposition with OXA-23 (PDB code 4JF4) and OXA-13 (PDB code 1HY8). Potential rotamers for Trp222 were determined by a local optimization of the side chain with meropenem fixed in the active site. A nearest neighbors (with 5 Å) calculation based on the initial position of meropenem in each Trp222 rotamer variant of OXA-51 was used to identify and define the receptor target region for flexible docking of meropenem to each of the Trp222 rotamer variants. All modeling, flexible docking and structure analyses were achieved using ICM-Pro 3.8-0.[9,10]

Supplemental Figures

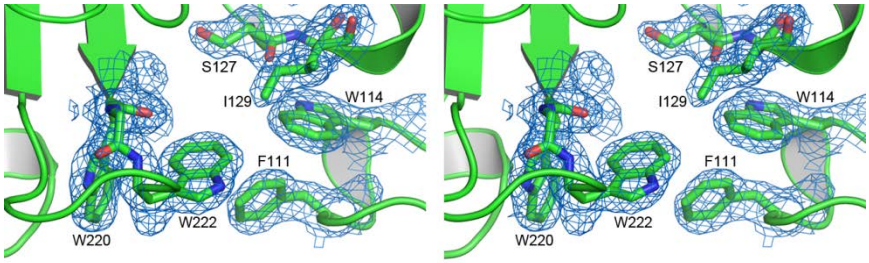

Figure S1. Final electron density map for OXA-51. Stereoview of the final $2F_o$-F_c electron density (blue) contoured at 1σ, near the opening of the active site of the apo OXA-51 structure (green).

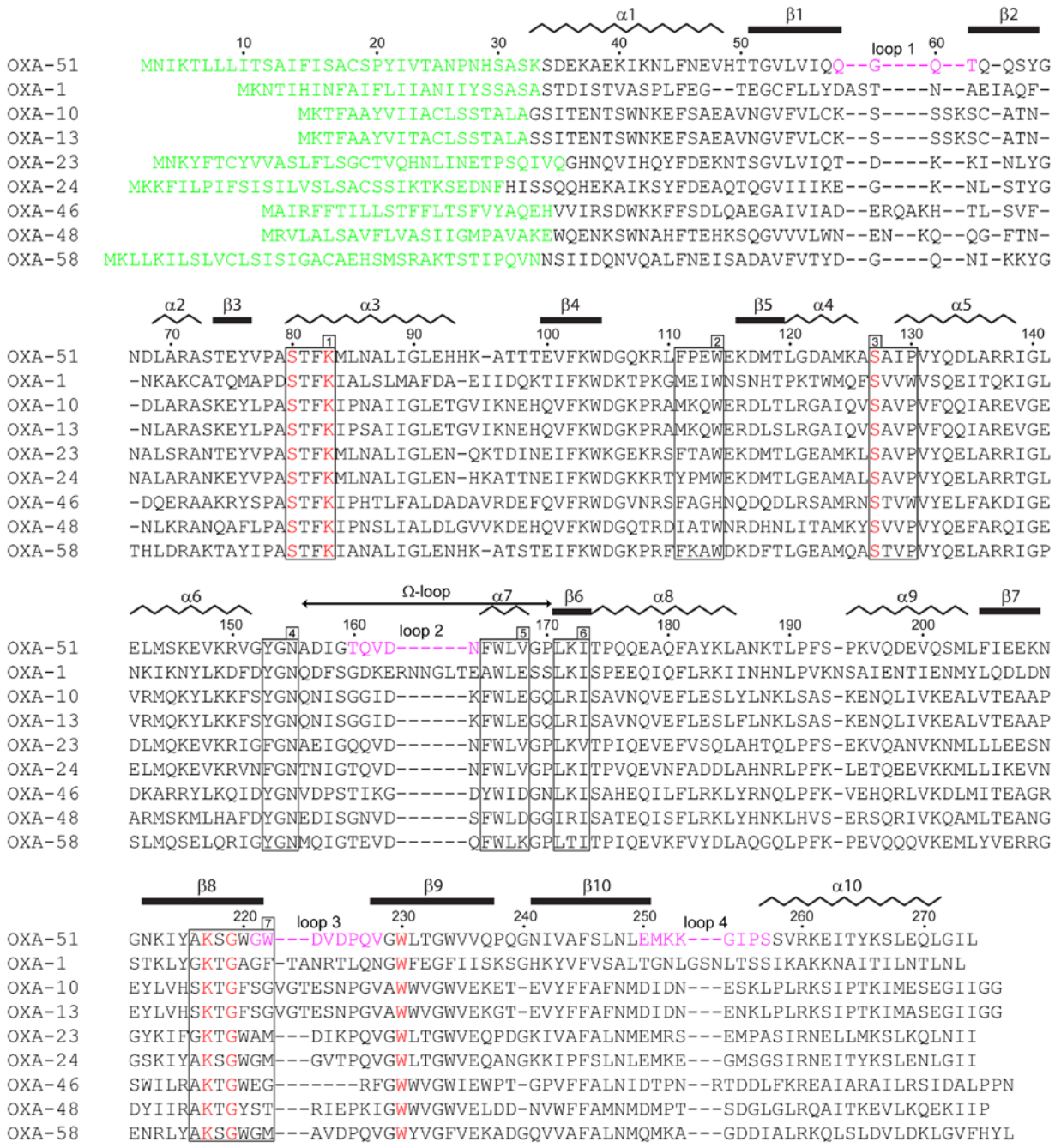

Figure S2. Structure-based sequence alignment of OXA-51 with eight published OXA enzymes structures. The secondary structure elements for OXA-51 are indicated above the sequence, along with the amino acid numbers. The residues colored green are not observed in the nine structures. Seven conserved sequence motifs, identified from an alignment of all known OXA sequences, are indicated by rectagular boxes and numbers in squares. Six residues identified as

being universally conserved in all the known OXA sequences are colored red. The four variable loop identified from superpositions of OXA-51 with other OXA enzyme structures, and colored magenta on the OXA-51 sequence, and labeled as loops 1 - 4.

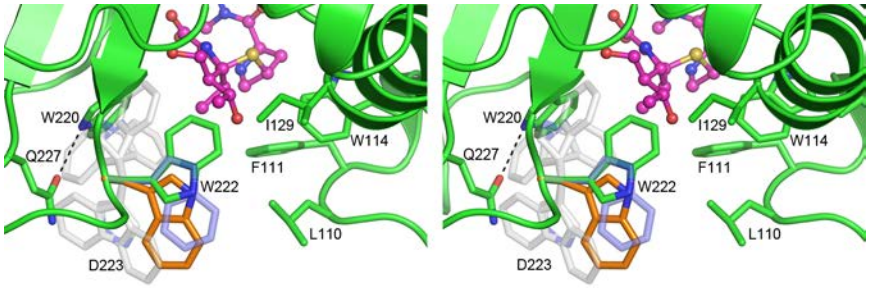

Figure S3. The alternate rotamers of Trp222. Stereoview of the alternate conformation of Trp222 (orange sticks) from energy minimization calculations, which would allow for the binding of a carbapenem substrate (magenta ball-and-sticks) in the OXA-51 active site (green) and still maintain some hydrophobic interactions with Leu110 and Phe111. The closest rotamer from COOT is shown as semi-transparent blue sticks. Five other rotamer conformations for the tryptophan residue, inaccessible due to unfavorably interactions with Trp220, Gln227 and other parts of the protein molecule, are also indicated as semi-transparent grey sticks.

Supplemental Tables

Table S1. Comparison of *A. baumannii* OXA-51 with other class D β-lactamase structures

	PDB code	Sequence identity (%) [a]	*rmsd* (Å) all Cα [b]	Bacterial source
OXA-1	3isg	25.4	1.5 (224)	*Escherichia coli*
OXA-2	1k38	31.5	1.4 (220)	*Salmonella typhimurium*
OXA-10	1ewz	35.8	1.4 (227)	*Pseudomonas aeruginosa*
OXA-13	1h8y	33.6	1.4 (230)	*P. aeruginosa*
OXA-23	4jf4	63.4	0.6 (238)	*A. baumannii*
OXA-24	3g4p	66.8	0.6 (240)	*A. baumannii*
OXA-45	4gn2	26.0	1.8 (207)	*P. aeruginosa*
OXA-46	3if6	31.1	1.4 (211)	*P. aeruginosa*
OXA-48	3hbr	37.3	1.2 (225)	*Klebsiella pneumonia*
OXA-58	4oh0	54.2	0.8 (240)	*A. baumannii*
OXA-146	4k0w	63.0	0.7 (227)	*A. baumannii*

[a] Calculated by the SSM algorithm as implemented in COOT.[6] [b] Values in parentheses give the total number of Cα atoms matched.

Table S2. Fully and partially conserved residues in the active site of the OXA enzymes

Motif [a]	OXA-51-like	Other OXA[b]	Role of conserved residue
1	**S**TF**K**	STFK	
	Ser80	**Ser** (100%)	Nucleophile for attack of the β-lactam ring
	Lys83	**Lys** (100%)	Carboxylated
2	**F**PE**W**	FPAW	
	Phe111	Phe (51%)	Hydrophobic interaction with substrate
	Trp114	Trp (88%)	Hydrophobic interaction with substrate
3	**S**A**I**	SAV	
	Ser127	**Ser** (100%)	Hydrogen bond to substrate and Lys217
	Ile129	Val (88%)	Hydrophobic interaction with Leu167[c]
5	F**WL**V	FWLV	
	Trp166	Trp (97%)	Hydrogen bond to carboxylated Lys83
	Leu167	Leu (82%)	Hydrophobic interaction with Ile129[c]
7	A**K**S**GW**G**W**	AKTGWGM	
	Lys217	**Lys** (100%)	Hydrogen bond to Ser127
	Gly219	**Gly** (100%)	
	Trp220	Trp (59%)	Forms wall of active site
	Trp222	Met (35%)	Interaction with Leu110 and Phe111

[a] The structural motifs are described as for the OXA-58 structure.[11] [b] Residue names in bold are completely conserved in all known class D β-lactamases. [c] It has been postulated that this interaction may be important in opening and closing a channel for the deacylating water molecule to enter the active site from the external milieu.[1]

Table S3, related to Figure 1: Diffraction Data Collection Statistics

Maximum resolution (d_{min}) (Å)	2.0
Observed reflections	128042
Unique reflections to d_{min}	20085
R_{sym} (%)	4.3 (75.5)[a]
I/σ	26.4 (2.5)
Completeness (%)	99.7 (99.6)
CC½ [b]	100.0 (77.9)
Multiplicity	6.4
Wilson B ($Å^2$)	36.5
Unit cell dimensions	
a = b(Å)	131.11
c (Å)	67.53

[a] Numbers in parentheses relate to the highest resolution shell, 2.05 – 2.00 Å. [b] Percentage of correlation between intensities from random half-sets of data.[12]

Table S4, related to Figure 1: OXA-51 Structure Refinement Statistics

Resolution range (Å)		33.8 – 2.0
R-factor / R_{free} (%)[a]		15.7 / 21.6
R_{all} (%)[b]		16.0
Total atoms - protein / solvent		1906 / 147
B factors	- protein chain ($Å^2$)	42.4
	- solvent ($Å^2$)	49.0
rms deviation from ideality		
	- bonds (Å)	0.007
	- 1-3 distances (Å)	1.02
Ramachandran plot		
	- residues in most favored regions (%)	97.5
Molprobity Overall Score [c]		1.25

[a] $R = \Sigma||F_o| - k|F_c|| / \Sigma|F_o| \times 100$. R_{free} was calculated with 5% of the reflections. [b] Final R-factor calculated with all data using no sigma cutoff. [c] The overall score represents the expected resolution for a model of the same quality.[13]

SUPPORTING REFERENCES

(1) Smith, C. A., Antunes, N. T., Stewart, N. K., Toth, M., Kumarasiri, M., Chang, M., Mobashery, S., and Vakulenko, S. B. (2013) Structural basis for carbapenemase activity of the OXA-23 β-lactamase from *Acinetobacter baumannii*. *Chem. Biol. 20*, 1107–1115.

(2) Matthews, B. W. (1968) Solvent contents of protein crystals. *Journal of Molecular Biology 33*, 491–497.

(3) Kabsch, W. (1993) Automatic processing of rotation diffraction data from crystals of initially unknown symmetry and cell constants. *J. Appl. Crystallogr. 26*, 795–800.

(4) Winn, M. D., Ballard, C. C., Cowtan, K. D., Dodson, E. J., Emsley, P., Evans, P. R., Keegan, R. M., Krissinel, E. B., Leslie, A. G. W., McCoy, A., McNicholas, S. J., Murshudov, G. N., Pannu, N. S., Potterton, E. A., Powell, H. R., Read, R. J., Alexei Vagin, A., and Wilson, K. S. (2011) Overview of the CCP4 suite and current developments. *Acta Cryst. D67*, 235–242.

(5) Adams, P. D., Afonine, P. V., Bunkóczi, G., Chen, V. B., Davis, I. W., Echols, N., Headd, J. J., Hung, L. W., Kapral, G. J., Grosse-Kunstleve, R. W., McCoy, A. J., Moriarty, N. W., Oeffner, R., Read, R. J., Richardson, D. C., Richardson, J. S., Terwilliger, T. C., and Zwart, P. H. (2010) PHENIX: A comprehensive Python-based system for macromolecular structure solution. *Acta Crystallogr. D66*, 213–221.

(6) Emsley, P., and Cowtan, K. (2004) Coot: Model-building tools for molecular graphics. *Acta Crystallogr. D60*, 2126-2132.

(7) Krissinel, E., and Henrick, K. (2004) Secondary-structure matching (SSM), a new tool for fast protein structure alignment in three dimensions. *Acta Crystallogr. D60*, 2256–2268.

(8) DeLano, W. L. *The PyMOL Molecular Graphics System*, San Carlos, CA, 2002.

(9) Schapira, M., Abagyan, R., and Totrov, M. (2003) Nuclear hormone receptor targeted virtual screening. *J. Med. Chem. 46*, 3045–3059.

(10) Schapira, M., Raaka, B. M., Das, S., Fan, L., Totrov, M., Zhou, Z., Wilson, S. R., Abagyan, R., and Samuels, H. H. (2003) Discovery of diverse thyroid hormone receptor antagonists by high-throughput docking. *Proc. Natl. Acad. Sci. 100*, 7354–7359.

(11) Smith, C. A., Antunes, N. T., Toth, M., and Vakulenko, S. B. (2014) Crystal Structure of Carbapenemase OXA-58 from *Acinetobacter baumannii*. *Antimicrob. Agents Chemother. 58*, 2135–2143.

(12) Karplus, P. A., and Diederichs, K. (2012) Linking crystallographic model and data quality. *Science 336*, 1030–1033.

(13) Chen, V. B., Arendall, W. B., Headd, J. J., Keedy, D. A., Immormino, R. M., Kapral, G. J., Murray, L. W., Richardson, J. S., and Richardson, D. C. (2010) MolProbity: All-atom structure validation for macromolecular crystallography. *Acta Crystallogr. D66*, 12–21.